


Young Leaf White Stripe encodes a P-type PPR protein required for chloroplast development

Jie Lan^{1†}, Qibing Lin^{2†}, Chunlei Zhou^{1†}, Xi Liu¹, Rong Miao¹, Tengfei Ma¹, Yaping Chen¹, Changling Mou¹, Ruonan Jing¹, Miao Feng², Thanhliem Nguyen¹, Yulong Ren², Zhijun Cheng², Xin Zhang², Shijia Liu¹, Ling Jiang^{1*} and Jianmin Wan^{1,2*} 

1. State Key Laboratory of Crop Genetics and Germplasm Enhancement, Jiangsu Plant Gene Engineering Research Center, Nanjing Agricultural University, Nanjing 210095, China

2. National Key Facility for Crop Gene Resources and Genetic Improvement, Institute of Crop Science, Chinese Academy of Agricultural Sciences, Beijing 100081, China

[†]These authors contributed equally to this work.

*Correspondences: Jianmin Wan (wanjm@njau.edu.cn); Dr. Wan is responsible for the distribution of the materials associated with this article); and Ling Jiang (jiangling@njau.edu.cn)



Jie Lan



Jianmin Wan

ABSTRACT

Pentatricopeptide repeat (PPR) proteins function in post-transcriptional regulation of organellar gene expression. Although several PPR proteins are known to function in chloroplast development in rice (*Oryza sativa*), the detailed molecular functions of many PPR proteins remain unclear. Here, we characterized a rice *young leaf white stripe* (*ylws*) mutant, which has defective chloroplast development during early seedling growth.

Map-based cloning revealed that *YLWS* encodes a novel P-type chloroplast-targeted PPR protein with 11 PPR motifs. Further expression analyses showed that many nuclear- and plastid-encoded genes in the *ylws* mutant were significantly changed at the RNA and protein levels. The *ylws* mutant was impaired in chloroplast ribosome biogenesis and chloroplast development under low-temperature conditions. The *ylws* mutation causes defects in the splicing of *atpF*, *ndhA*, *rpl2*, and *rps12*, and editing of *ndhA*, *ndhB*, and *rps14* transcripts. *YLWS* directly binds to specific sites in the *atpF*, *ndhA*, and *rpl2* pre-mRNAs. Our results suggest that *YLWS* participates in chloroplast RNA group II intron splicing and plays an important role in chloroplast development during early leaf development.

Keywords: chloroplast development, PPR protein, ribosome biogenesis, RNA splicing

Lan, J., Lin, Q., Zhou, C., Liu, X., Miao, R., Ma, T., Chen, Y., Mou, C., Jing, R., Feng, M., et al. (2023). *Young Leaf White Stripe* encodes a P-type PPR protein required for chloroplast development. *J. Integr. Plant Biol.* **00**: 1–16.

INTRODUCTION

The chloroplast, a semiautonomous organelle that arose from a single endosymbiotic event between a photosynthetic cyanobacterium and a eukaryotic host, retains its own genome and gene translation system (Moreira et al., 2000; Sugimoto et al., 2004). Chloroplasts are essential for plant growth and development, providing energy for respiration and other physiological activities by fixing carbon and releasing oxygen. The chloroplast functions not only as a central metabolic hub but also as an environmental sensor

that perceives stress and produces retrograde signals to coordinate nuclear-encoded adaptive responses (de Souza et al., 2017).

Chloroplast development is dependent on the coordinated expression of nuclear and chloroplast genes. Post-transcriptional RNA modifications, such as RNA cleavage, splicing, editing, and stabilization, usually occur during the expression of these genes, and many RNA-binding proteins are involved in these RNA modifications (Shikanai and Fujii, 2013). Since the nuclear genome encodes >90% of all chloroplast proteins and chloroplast development requires

the coordinated expression of nuclear and plastid genes, cloning and characterizing more nuclear-encoded RNA-binding proteins should help to reveal the mechanisms regulating gene expression during chloroplast development.

Pentatricopeptide repeat (PPR) proteins are RNA-binding proteins that function in RNA splicing, editing, stability, maturation, and translation (Hammani et al., 2016; Zoschke et al., 2016; Liu et al., 2018). In land plants, the large family of PPR proteins has more than 450 members in *Arabidopsis thaliana* and 491 in rice (*Oryza sativa*). These proteins are divided into P and PLS subfamilies according to the composition of tandem arrays of a degenerate 35-amino acid motif (O'Toole et al., 2008). P-class proteins consist of tandem arrays of a single type of PPR motif (the P motif) and have roles in RNA binding, splicing, stabilization, and translation. The PLS subfamily contains tandem arrays of the classical PPR motifs P (35 amino acids), PPR-like L (long, 35 or 36 amino acids), and PPR-like S (short, 31 amino acids) that mainly function as RNA editing proteins (Lurin et al., 2004; Barkan et al., 2012). Although many nuclear-encoded PPR proteins are responsible for post-transcriptional modulation of gene transcripts in *Arabidopsis*, the functions of only a few members have been reported in rice. Among them, the mitochondrion-located P-type proteins FLOURY ENDOSPERM10 (FLO10) and FLO18 regulate *nad1* and *nad5* intron splicing, respectively (Wu et al., 2019; Yu et al., 2021), whereas the PLS-type proteins OPAQUE AND GROWTH RETARDATION1 (OGR1) and MITOCHONDRIAL PPR25 (MPR25) participate in mitochondrial RNA editing (Kim et al., 2009; Toda et al., 2012). Several chloroplast-located PPRs, such as YOUNG SEEDLING ALBINO (YSA) (Su et al., 2012), VIRESCENT4 (OsV4) (Gong et al., 2014), WHITE STRIPE LEAF (WSL) (Tan et al., 2014), PLASTID TRANSCRIPTIONALLY ACTIVE CHROMOSOME PROTEIN2 (OspTAC2) (Wang et al., 2016), and WHITE STRIPE LEAF5 (WSL5) (Liu et al., 2018), were reported to function in RNA editing and RNA splicing and thereby affect chloroplast development. Loss of function of the PLS-type protein WSL strongly affects the splicing of *rpl2*, leading to an albino phenotype (Tan et al., 2014), and the PLS-type protein OsPPR6 is involved in *ndhB* editing and *ycf3* splicing (Tang et al., 2017). P-type WSL5 targets chloroplasts and plays an essential role in splicing *rpl2* and *rps12* introns (Liu et al., 2018). However, the detailed functions of most PPR proteins remain unclear, and intensive studies of these proteins are needed to expand our understanding of the post-transcriptional regulation of plastid genes in rice.

In this study, we identified a rice mutant with white-striped leaves and impaired chloroplast structure during early seedling development and named the mutant *young leaf white stripe* (*ylws*). *YLWS* encodes a P-type PPR protein, which targets the chloroplast. Compared with the wild-type (WT), the *ylws* mutant had reduced expression of photosynthesis-related and plastid-encoded genes involved in chloroplast development. The *ylws* mutant is defective in splicing of *atpF*, *ndhA*, *rpl2*, and *rps12*, and editing of *ndhA*, *ndhB*, and *rps14*

transcripts. In addition, we found that *YLWS* directly binds to specific sites in *rpl2*, *ndhA*, and *atpF* pre-mRNAs. Our results suggest that *YLWS* could be involved in chloroplast development by affecting RNA splicing during early seedling development.

RESULTS

Phenotypic characterization of the *ylws* mutant

The *ylws* mutant was isolated from an ethyl methanesulfonate (EMS)-mutagenized population of *indica* rice cultivar Nanjing 11 (NJ11, WT). The *ylws* mutant exhibited a white-striped leaf phenotype during the two- to four-leaf growth stage (Figure 1A, B), after which the leaves gradually became green with no apparent difference from the WT (Figure 1C). The chlorophyll (Chl *a* and Chl *b*) and carotenoid contents at the three-leaf stage were significantly reduced in the *ylws* mutant compared with the WT (Figure 1D).

To test whether the *ylws* mutant phenotype is sensitive to temperature, we grew the WT and *ylws* mutant in a growth chamber at 20, 25, or 30°C and measured the chlorophyll contents. The *ylws* plants showed more extreme symptoms with severely decreased chlorophyll contents at 20°C (Figure 1E, F), moderate white stripes with moderately reduced chlorophyll content at 25°C (Figure 1E, G), and a pale-green phenotype with only slightly reduced chlorophyll content at 30°C (Figure 1E, H). These results showed that the *ylws* mutant is temperature sensitive.

The *ylws* mutant shows disrupted chloroplast development

We performed transmission electron microscopy (TEM) analysis of chloroplasts to examine whether ultrastructural changes occurred in the *ylws* mutant. Mesophyll cells of WT plants showed normal, well structured chloroplasts (Figure 2A, B). Chloroplasts from green portions of *ylws* mutant leaves were indistinguishable from those of the WT (Figure 2C), whereas chloroplasts from white sectors of mutant leaves had abnormal structures, including vacuolated plastids and lack of structurally organized, stacked thylakoid membranes (Figure 2D–F). These results suggested that the white-stripe leaf phenotype resulted from defective chloroplasts and that *YLWS* is required for chloroplast development during the early seedling stage.

Map-based cloning of *YLWS*

Genetic analysis of an F₂ population from a cross between the WT and *ylws* mutant showed that the *ylws* phenotype was conferred by a single recessive nuclear gene (Table S1). Twenty F₂ individuals with the *ylws* phenotype derived from a cross between the *ylws* mutant and *japonica* line 02428 were used in linkage analysis to establish the chromosome location. The *YLWS* locus was associated with the simple sequence repeat (SSR) markers N3-17 and N3-22 on the short arm of chromosome 3. Further fine mapping using 983 F₂

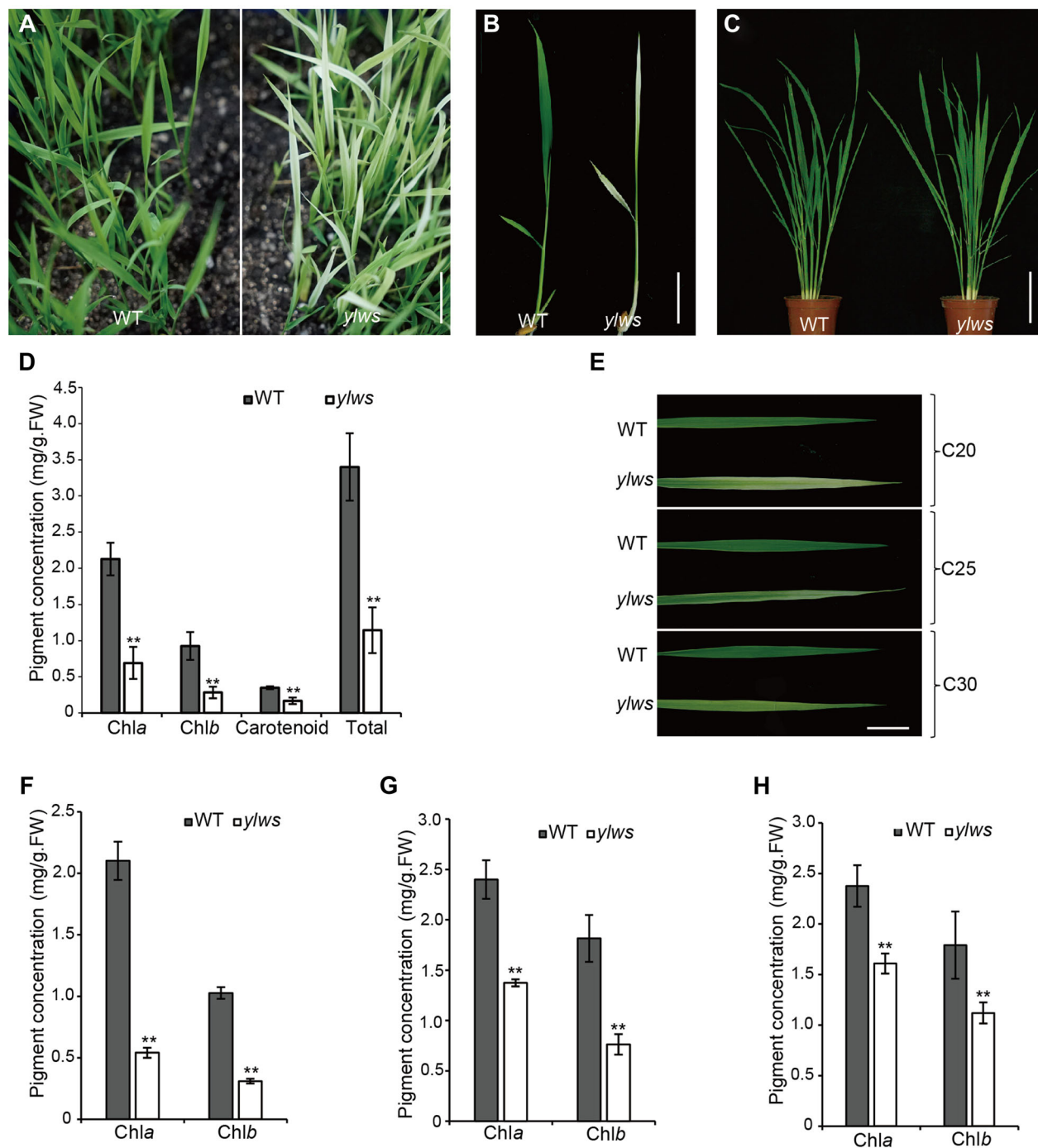


Figure 1. Phenotypes of the *y/lws* mutant

(A) Phenotypes of wild-type (WT, left) and *y/lws* mutant (right) seedlings 15 d post planting and grown at 20°C. Bar, 2 cm. (B) Phenotypes of WT (left) and *y/lws* mutant (right) at the second leaf stage. Bar, 3 cm. (C) Phenotypes of WT (left) and *y/lws* mutant (right) at the tillering stage. Bar, 15 cm. (D) Leaf pigment concentrations of field-grown WT and *y/lws* mutant seedlings at 15 d post seeding. Chl a, chlorophyll a; Chl b, chlorophyll b; Car, carotenoids. (E) Leaves of WT and *y/lws* mutant seedlings grown at 20°C, 25°C, and 30°C. Bar, 2 cm. (F–H) Leaf pigment concentrations of WT and *y/lws* mutant seedlings at the three-leaf stage when grown at 20°C (F), 25°C (G), and 30°C (H), respectively. Values are means \pm SD from three independent repeats. Student's *t*-tests: ***P* < 0.01. FW, fresh weight.

individuals with mutant phenotype narrowed the *YLWS* locus to a 148-kb interval between markers L10 and L22 containing 14 open reading frames (ORFs) (Figure 3A). Sequencing analysis of all 14 ORFs revealed that compared with the WT, ORF5 (*Os03g0309800*) had an 8-bp deletion in its coding

region, causing a premature stop codon (Figure 3B). The mutant site was further confirmed by SSR analysis using an insertion/deletion (InDel) marker pair (Figure 3C). These results suggested that *Os03g0309800* was the candidate gene corresponding to the *YLWS* locus.

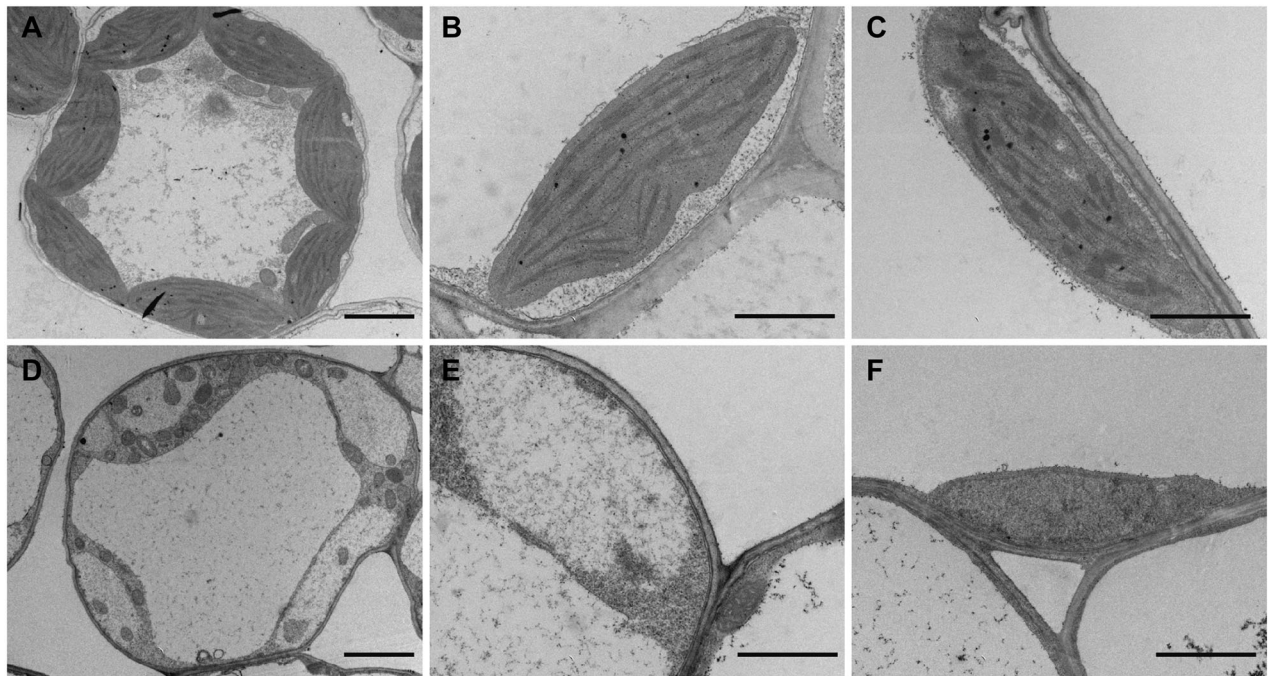


Figure 2. Transmission electron micrographs of mesophyll cells from WT and *y/lws* mutant leaves

(A) and (B) Chloroplasts from WT leaves at the three-leaf stage. (C) Chloroplasts from green portions and (D–F) white sectors of the same *y/lws* mutant leaves. Bars, 2 μm in (A) and (D), 1 μm in (B), (C), (E), and (F). WT, wild-type.

To verify whether the 8-bp deletion in *Os03g0309800* was responsible for the *y/lws* phenotype, we transformed a 4-kb WT genomic fragment of *Os03g0309800* into the *y/lws* mutant. As expected, positive transgenic seedlings had normal leaf color (Figure 3D). Positive transgenic knockout mutants produced by clustered regularly interspaced short palindromic repeats (CRISPR)/CRISPR-associated protein 9 (Cas9) gene editing in rice cultivar Kitaake showed similar seedling phenotypes to the *y/lws* mutant (Figure 3E, F). Taken together, these results confirmed that *Os03g0309800* was the *YLWS* locus.

YLWS encodes a chloroplast-targeted P-type PPR protein

Sequence analysis revealed that *YLWS* encodes a PPR protein of 540 amino acids (<https://blast.ncbi.nlm.nih.gov>), with putative homologs in maize (*Zea mays*) and Arabidopsis (Figure S1) (Williams and Barkan, 2003; Lu et al., 2011). *YLWS* contains 11 canonical PPR motifs according to motif prediction by TPRpred (<https://toolkit.tuebingen.mpg.de/tools/tpred>) and was thus identified as a P-type PPR protein (Figure 4A, B).

Based on TargetP analysis (<http://www.cbs.dtu.dk/services/TargetP>), *YLWS* has a putative chloroplast localization signal at the N terminus (Figure 4A). To test this prediction, we expressed a *YLWS*-green fluorescent protein (GFP) fusion protein in rice protoplasts and found that the GFP fluorescence of *YLWS*-GFP displayed some dot-like structures which overlapped the chloroplast autofluorescence (Figure 4C). These dot-like structures seemed to be localized in chloroplast nucleoids which can be marked by YSS1, a chloroplast nucleoid-located protein

(Zhou et al., 2017). We therefore constructed YSS1-mCherry as a nucleoid marker to perform colocalization analyses of *YLWS* and YSS1. As shown in Figure 4D, *YLWS* was localized in the chloroplast nucleoids.

Real-time quantitative reverse transcription polymerase chain reaction (RT-qPCR) analysis showed that *YLWS* was expressed in various tissues, and expression levels in L4 leaves of seedlings and young leaves of adult plants were more than in other tissues (Figures 4E, F, S2), consistent with data from the Rice eFP Browser (<http://bar.utoronto.ca/efp/price/cgi-bin/efpWeb.cgi>). The strongest expression of *YLWS* in young leaves, such as L4 leaves, corresponded to an important stage in early chloroplast development, during which the *y/lws* mutant displayed the white-striped leaf phenotype. We also analyzed *YLWS* expression in WT plants grown at 20°C and 30°C. The transcript abundances of *YLWS* at the three-leaf stage were higher in the WT under low temperatures (Figure 4G). These results, together with the different phenotypes at 20°C and 30°C (Figure 1E), indicated that *YLWS* is induced by low temperatures and plays an essential role in early chloroplast development under low temperatures.

The *y/lws* mutant is defective in RNA splicing of chloroplast group II introns

Many characterized PPR proteins participate in chloroplast RNA splicing and editing (Cai et al., 2017; Zhang et al., 2017; Liu et al., 2018; Liu et al., 2021). To test whether *YLWS* also played a role in chloroplast RNA splicing, we performed reverse transcription PCR (RT-PCR) using specific primers listed

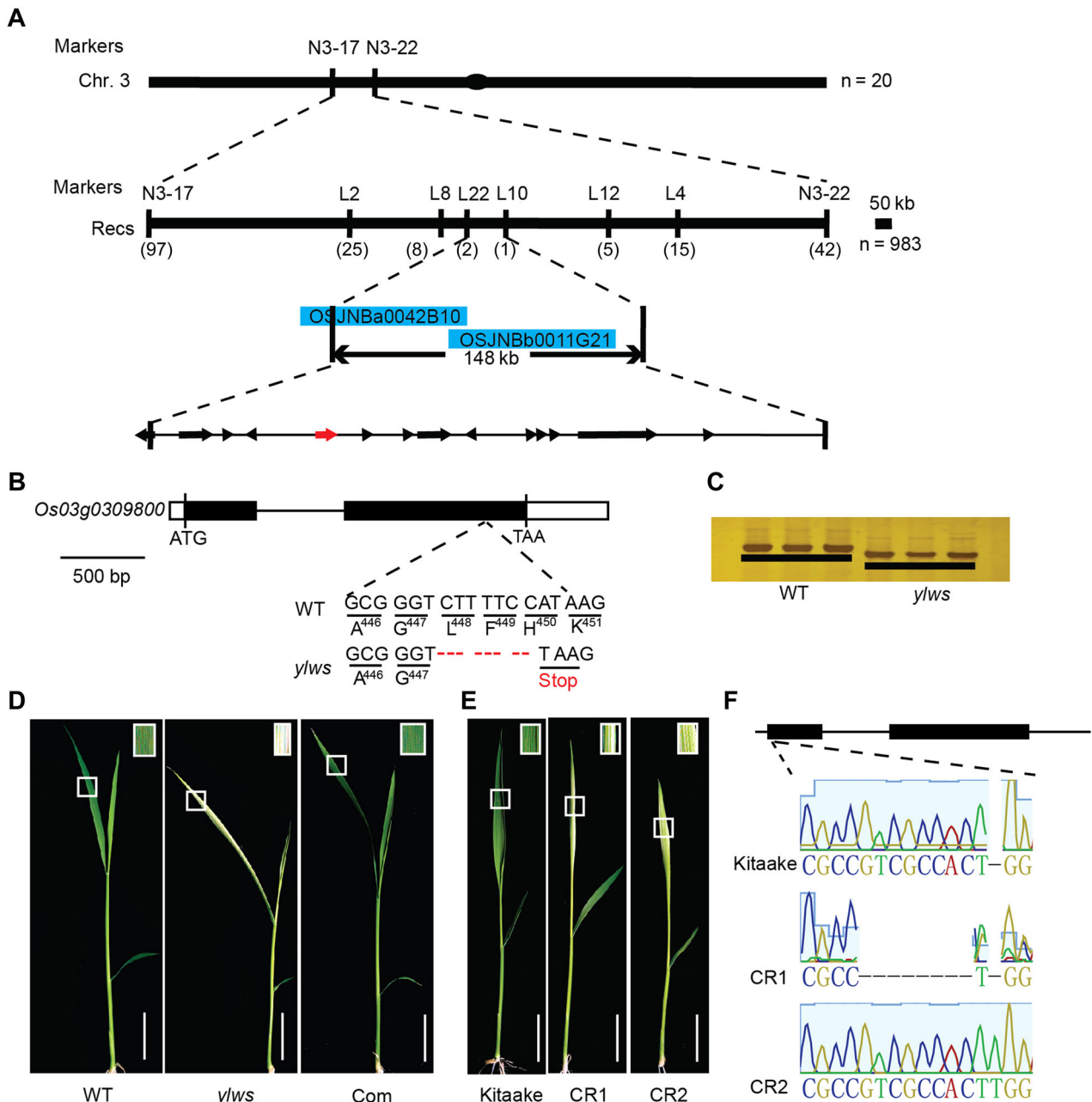


Figure 3. Map-based cloning of the *y/lws* locus

(A) The *y/lws* locus was fine mapped to a 148-kb interval between markers L22 and L10 on chromosome 3 (Chr. 3). Arrows represent 14 putative genes in the region. The *y/lws* locus is indicated by a red arrow. (B) Structure of *YLWS* and *y/lws*. Black boxes indicate the exons, and the white boxes indicate the 5'UTR and 3'UTR. ATG and TAA are the start and stop codons. An 8-bp deletion in *y/lws* causes premature termination of translation after 447 amino acids. (C) Verification of the difference between the *YLWS* and *y/lws* genomic locus using a pair of InDel markers. (D) Complementation of *y/lws* by the wild-type *YLWS* allele. Bar, 3 cm. (E) Phenotypes of *YLWS* knock out lines in Kitaake. Bar, 3 cm. (F) Mutations at the target sites in *YLWS* knock out lines CR1 and CR2 generated by the CRISPR/Cas9. Filled bars indicate exons and lines represent introns of *YLWS*.

in Table S3. The rice chloroplast genome contains 18 introns, including 17 group II introns and one group I intron (Hiratsuka et al., 1989). All chloroplast transcripts were amplified using primers flanking the introns, and the lengths of the amplified products were compared between the WT and the *y/lws* mutant. Four transcripts, *atpF*, *rps12-intron2*, *ndhA*, and *rpl2*, containing group II introns had unspliced cDNA in the *y/lws* mutant

compared with the WT (Figure 5). This suggested that *YLWS* is essential for their splicing. As expected, the defective splicing was rescued in the complemented transgenic line and was present in the knockout transgenic line (Figure 6A).

To confirm splicing defects in the *y/lws* mutant, we performed RT-qPCR to compare the ratio of spliced/unspliced transcripts. The *y/lws* mutant had reduced efficiency in *atpF*,

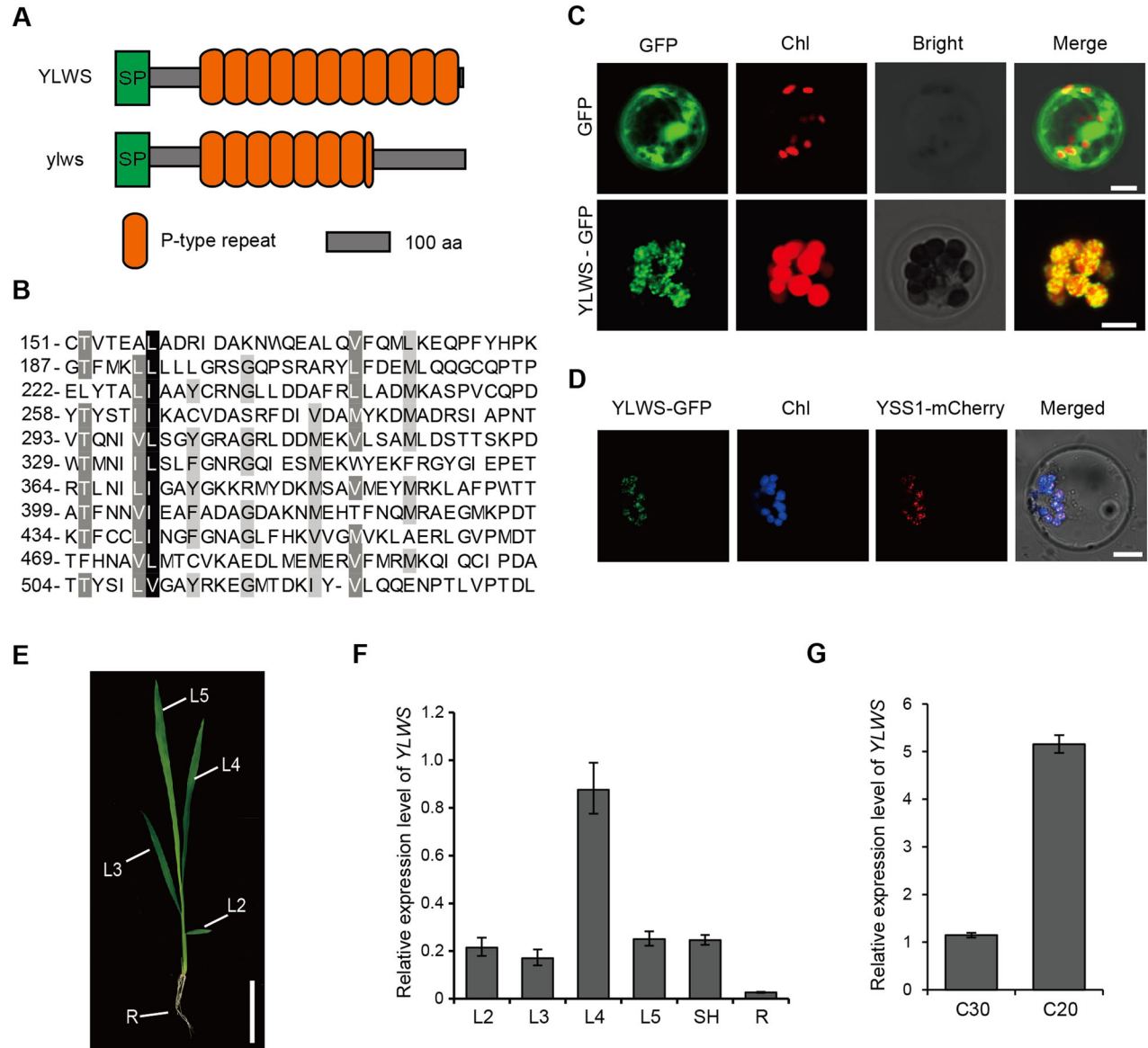


Figure 4. Subcellular localization of YLWS and expression analysis of YLWS

(A) Schematic structure of the functional domains of YLWS. SP, signal peptide predicted by TargetP. (B) The 11 PPR motifs of YLWS. (C) Subcellular localization of YLWS-GFP fusion protein in rice protoplasts. Bars, 10 μ m. (D) Colocalization of YLWS-GFP and YSS1-mCherry within chloroplast nucleoids. Bar, 10 μ m. (E) A rice seedling with fully expanded fifth leaf. Bar, 4 cm. (F) Transcript levels of YLWS in different tissues of WT seedlings. L2, second leaf, L3, third leaf, L4, fourth leaf, L5, fifth leaf, SH, sheath, R, root. (G) Transcript levels of YLWS in third leaves of WT seedlings at 30°C and 20°C. Values are means \pm SD ($n = 3$) in (F) and (G).

ndhA, *rpl2*, and *rps12* splicing compared with the WT (Figure 6B). To further confirm these splicing defects, we designed specific probes for the four transcripts for northern blotting (Figure 6C). As expected, unspliced precursors of the four transcripts were overaccumulated in the *ylws* mutant compared with the WT (Figure 6D). These results indicated that YLWS is essential for RNA splicing of chloroplast group II introns.

YLWS directly binds to *ndhA*, *atpF*, and *rpl2* pre-mRNAs

Given that *atpF*, *rps12*-intron2, *ndhA*, and *rpl2* splicing was impeded in the *ylws* mutant we predicted that YLWS would

bind to specific sites in their pre-mRNAs. Based on the PPR recognition code and previous reports (Barkan et al., 2012; Yagi et al., 2013), we predicted possible YLWS-binding sites using the MEME suite (<https://meme-suite.org/meme/index.html>) (Figures 7A, S3). We performed RNA electrophoretic mobility shift assays (REMSAs) to test our prediction. The purified recombinant YLWS-GST proteins were incubated with RNA probes for *rpl2*, *atpF*, and *ndhA* or an unlabeled competitive probe. YLWS-GST bound to the specific RNA nucleotides of *ndhA*, *rpl2*, and *atpF*, and the ability of YLWS binding to these pre-mRNAs was alleviated with

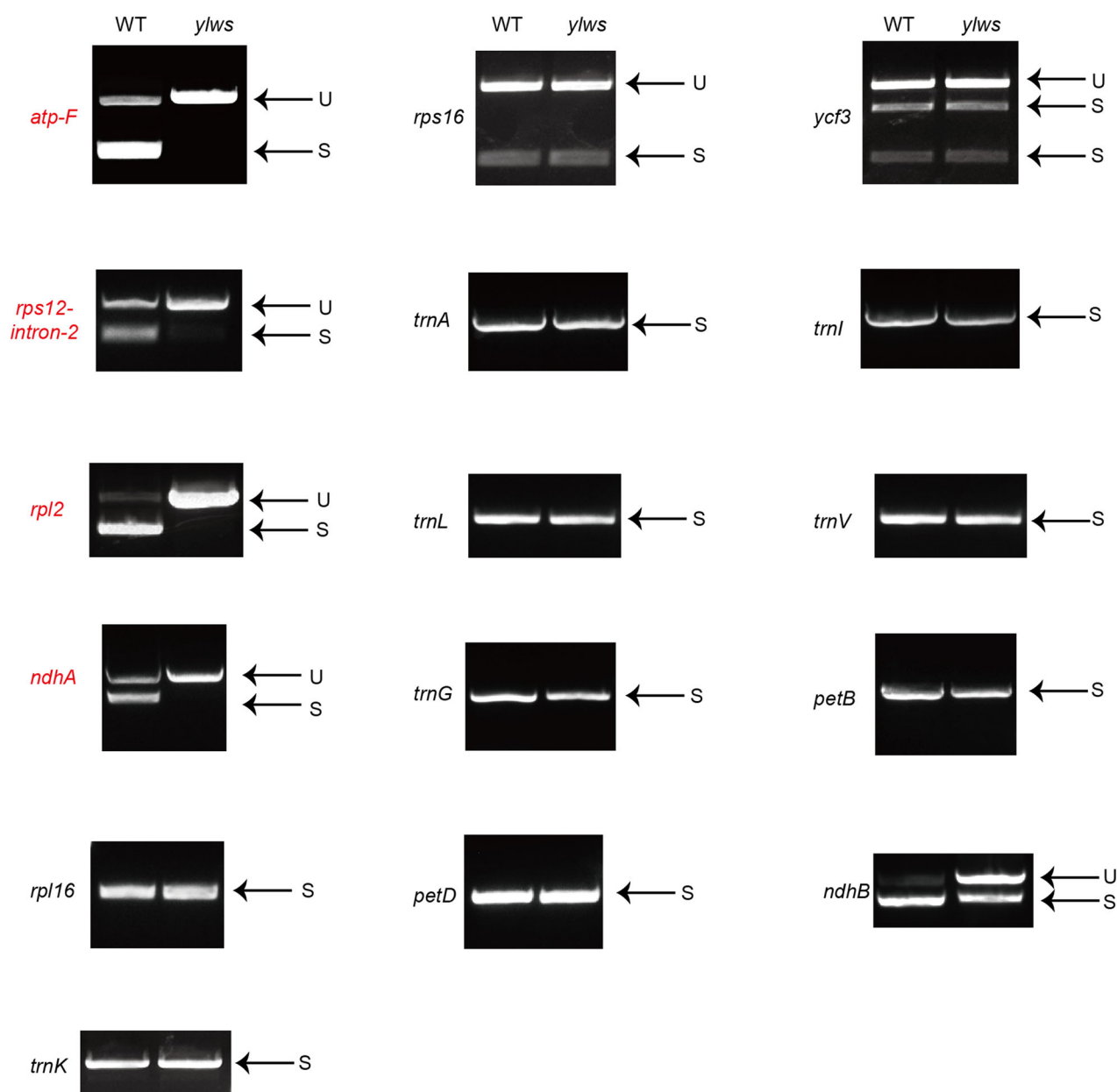


Figure 5. Splicing analyses of rice chloroplast transcripts in WT and *y/lws* mutant

Gene transcripts are labeled at the left. Spliced (S) and unspliced (U) transcripts are shown at the right. RNA was extracted from WT and *y/lws* mutant plants. WT, wild-type.

increased concentrations of competitive probes but not the unrelated probe (Figures 7B, S4; Table S3). RNA CoIP analysis in rice protoplasts showed that YLWS could be specifically recruited to the *rpl2*, *atpF-1*, *atpF-2*, *ndhA-1*, *ndhA-2*, and *ndhA-3* regions with most enrichment in the *rpl2*, *atpF-2*, and *ndhA-3* probe regions (Figure 7C–E).

Expression levels of chloroplast-associated genes are affected in the *y/lws* mutant

Chloroplast development is controlled by the transcription of plastid-encoded genes regulated by RNA polymerase complexes NEP and PEP (Pfalz et al., 2006). To address whether

YLWS influenced chloroplast gene expression we assayed the expression levels of plastid-encoded genes in the WT and *y/lws* mutant. RT-qPCR analysis showed that expression of PEP-dependent genes, such as *PsaA* and *PsbA* (encoding reaction center polypeptides of photosystem I or II), and *RbcL* (the large subunit of Rubisco), was significantly reduced, whereas that of NEP-dependent genes, such as PEP subunit genes (*rpoA*, *rpoB*, *rpoC1*, and *rpoC2*), was elevated in the *y/lws* mutant at 20°C (Figure 8A). The PEP complex is composed of four plastid-encoded core subunits (*rpoA*, *rpoB*, *rpoC1*, and *rpoC2*) and several nuclear-encoded proteins such as polymerase-associated proteins. Downregulation of PEP-dependent genes

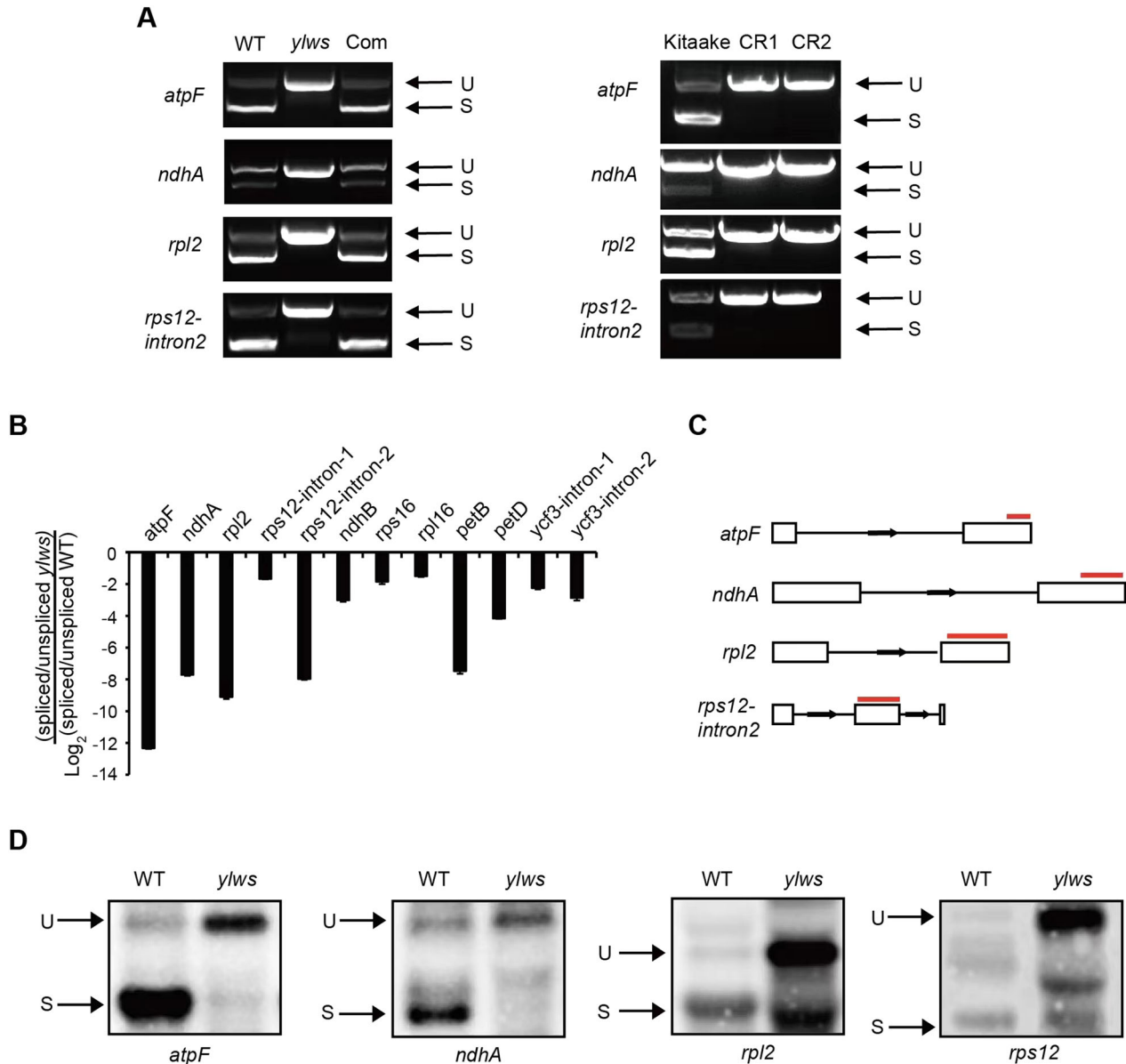


Figure 6. Splicing analyses of four chloroplast group II introns in WT and *ylws* mutant

(A) RT-PCR analyses of *atpF*, *ndhA*, *rpl2*, and *rps12* transcripts in WT, *ylws* mutant (white-striped sector), and complemented line (Com) (left panel) or Kitaake and knock out lines (white-striped sector) on the Kitaake background (right panel). **(B)** Quantitative RT-qPCR analyses of *atpF*, *ndhA*, *rpl2*, and *rps12* transcripts in WT, *ylws* mutant (white-striped sector). Values are means \pm SD ($n = 3$). **(C)** Sketch map of the *atpF*, *ndhA*, *rpl2*, and *rps12* transcripts. The red lines represent the probes used in **(D)**. **(D)** Northern blotting of *atpF*, *ndhA*, *rpl2*, and *rps12* splicing in the WT and *ylws* mutant. Positions of spliced (S) and unspliced (U) transcripts are shown by arrows in **(A)** and **(D)**. WT, wild-type.

and upregulation of NEP-associated genes usually imply defects in PEP complex activity (Chateigner-Boutin et al., 2011; Lv et al., 2017). These findings suggested that PEP complex activity was disrupted in the *ylws* mutant at 20°C.

We also determined transcript levels of key photosynthesis-associated nuclear genes and chlorophyll biosynthesis genes and found that the transcription of photosynthesis-associated nuclear genes *CAB1R*, *CAB2R*, and *RbcS* and chlorophyll biosynthesis genes *HEMA*, *HEML*, *HEMB*, *CHLD*, *HEME*, *CHLH*, *CHLM*, *CHLG*, *CRD*, and *POR*

was reduced in the *ylws* mutant at 20°C compared with the WT (Figure 8A, C). However, the expression level changes were less dramatic in the *ylws* mutant at 30°C (Figure 8B, D), consistent with the slight pale-green phenotype of the *ylws* mutant at 30°C.

Furthermore, we measured the abundance of photosynthetic proteins; Rubisco activase (RCA), Rubisco large subunit (RbcL), photosystem subunits PsaA and PsbA, and 50S ribosomal protein L2 (Rpl2) were lower in the *ylws* mutant than in the WT (Figure 8E, F). Rpl2 is a component of the

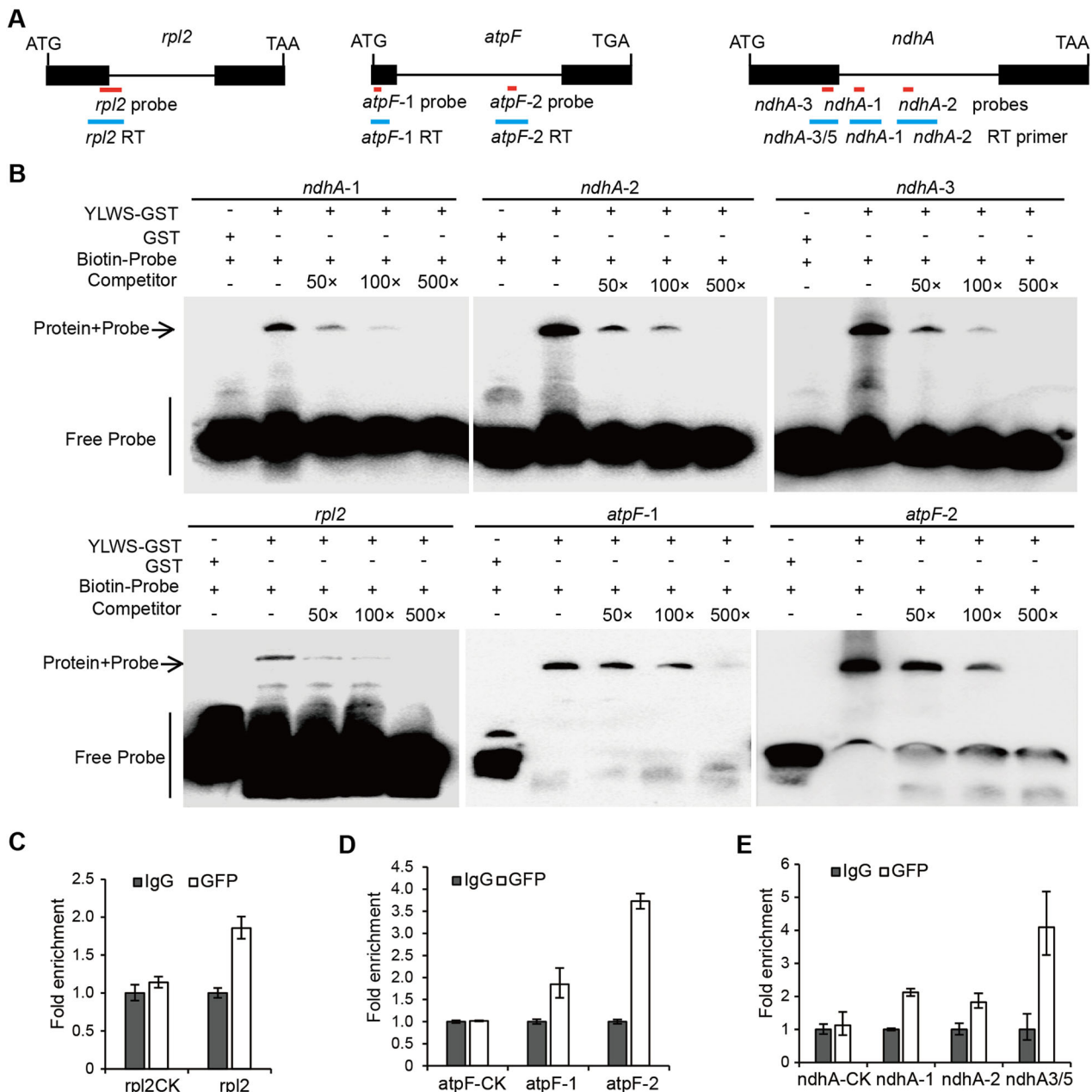


Figure 7. RNA electrophoretic mobility shift assay (REMSA) of YLWS

(A) Sketch diagram of the REMSA probes (red) and RNA CoIP primers (blue) for *rpl2*, *ndhA*, and *atpF* used in (C–E) on their corresponding pre-mRNAs. (B) REMSA analysis of YLWS-GST. Biotin-labeled specific *ndhA-1*, *ndhA-2*, *ndhA-3*, *rpl2*, *atpF-1*, and *atpF-2* RNA sequences were used as probes. YLWS-GST, GST, and biotin-labeled probes were present (+) or absent (-) in each reaction. GST protein was used as a negative control. Unlabeled probes were used as competitors. (C–E) RNA CoIP analyses of YLWS in rice protoplast. *rpl23*, *atpA*, and *ndhH* were used as *rpl2*-CK, *atpF*-CK, and *ndhA*-CK respectively. Values are means \pm SD ($n = 3$).

chloroplast ribosome that functions as the translation machinery for chloroplast proteins. The chloroplast ribosome is composed of a 50S large subunit and a 30S small subunit and, in detail, the two subunits are further composed of multiple rRNAs (16S, 23S, 5S, and 4.5S) and ribosomal proteins. To test if the chloroplast ribosome was impaired in the *y/lws* mutant, we analyzed the composition and contents of rRNAs in *y/lws* and WT plants using an Agilent 2100

bioanalyzer. The 16S and 23S chloroplast rRNA subunits were barely detected in white portions of the *y/lws* mutant leaves (Figure S5A), and the levels of 16S and 23S subunits in whole *y/lws* mutant leaves were substantially reduced compared with those in whole WT leaves in seedlings grown at 20°C (Figure S5B). However, these differences were much less dramatic between seedlings grown at 30°C (Figure S5C). YLWS is homologous with AtPPR2 (Figure S1), which binds

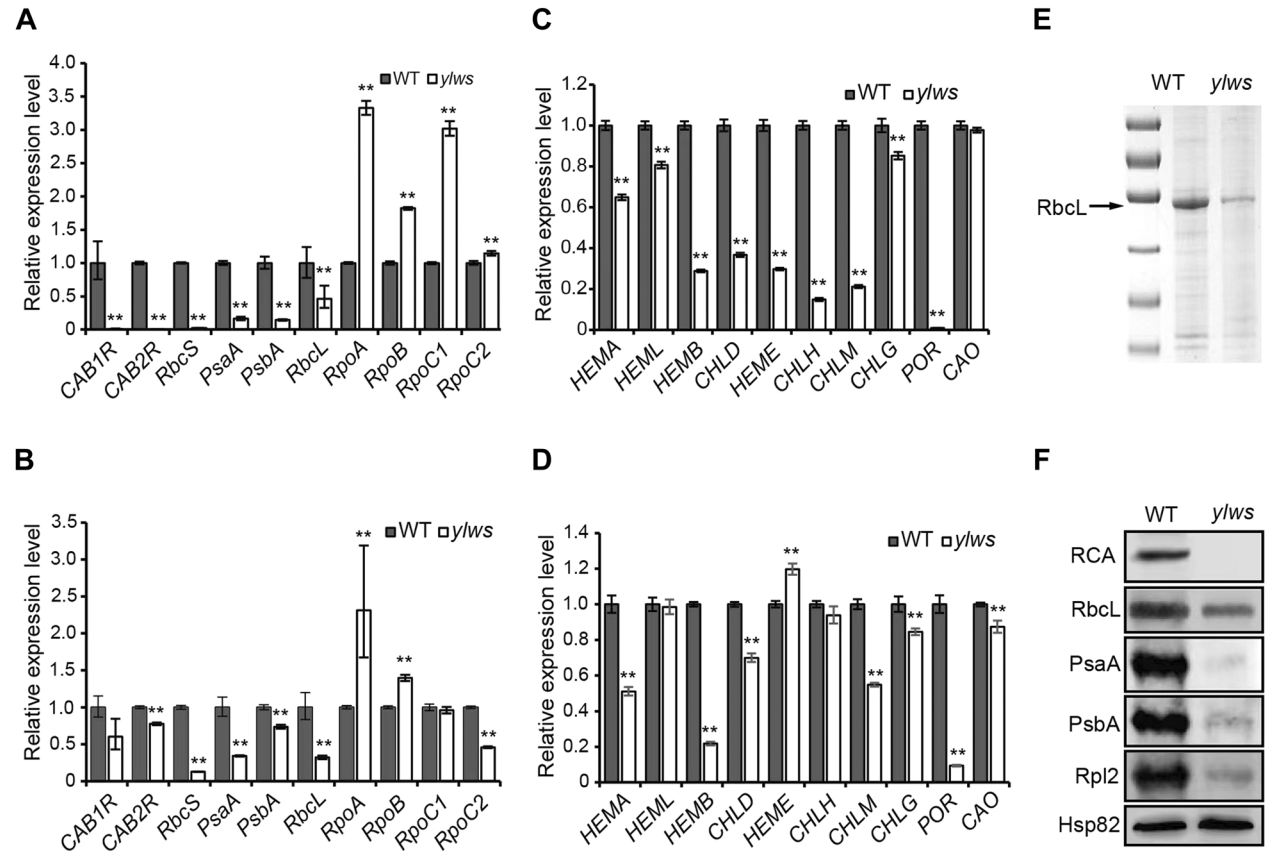


Figure 8. Expression levels of representative genes associated with chloroplasts

(A, B) RT-qPCR analysis of photosynthesis-associated genes in WT and *y/lws* mutant at the three-leaf stage grown at 20°C (A) and 30°C (B). (C, D) RT-qPCR analysis of chloroplast synthesis genes in WT and the *y/lws* mutant at the three-leaf stage grown at 20°C (C) and 30°C (D). Values are means \pm SD ($n = 3$). (E, F) Abundance of photosynthetic proteins of WT and the *y/lws* mutant at the three-leaf stage when grown at 20°C. Hsp82 was used as the internal reference. Student's *t*-tests: ** $P < 0.01$. WT, wild-type.

to plastid 23S rRNA and plays an important role in gametogenesis and embryogenesis (Lu et al., 2011). Therefore, we tested by RNA pull-down assay whether YLWS could bind to 23S rRNA. The results showed that YLWS could bind to biotin-labeled 23S rRNA *in vitro* (Figure S5D, E). We predicted possible target sites in 23S and performed REMSA analysis, but YLWS did not bind to the predicted sites (Figure S5F, G). These results confirmed that chloroplast ribosome biogenesis was severely impaired in the *y/lws* mutant seedlings grown at low temperatures.

The *y/lws* mutant is defective in RNA editing

RNA editing is an important post-transcriptional process that converts specific target cytidines to uridine to alter RNA sequences in plastids and mitochondria (Takenaka et al., 2013). Some PPRs were reported to participate in RNA editing (Hammani et al., 2009; Liu et al., 2018; Cui et al., 2019). To detect whether YLWS was involved in RNA editing, we sequenced all 21 identified RNA editing sites in chloroplast RNA. We found that the editing efficiencies of *ndhA*-C473, *ndhB*-C737, and *rps14*-C80 were reduced in the *y/lws* mutant and were restored to WT levels in the complemented line

(Figure S6A), whereas that of *rpoB* at C467, C545, and C560 was increased in *y/lws* compared with the WT (Figure S7). There was no obvious difference between WT and *y/lws* plants in the other 15 RNA editing sites (Figure S7; Table S2). C467 (codon 156), C545 (codon 182), and C560 (codon 187) of *rpoB* (encoding the β subunit of RNA polymerase) are located within the dispensable region, which can be deleted without altering the basic function of RNA polymerase in *Escherichia coli* (Corneille et al., 2000). Therefore, abnormal editing of *rpoB* sites may not be responsible for the white-striped phenotype of the *y/lws* mutant.

Next, we analyzed the sequences close to the target editing sites of *ndhA*, *ndhB*, and *rps14* transcripts and found nucleotides surrounding the target editing sites of *ndhA* that might be recognized by YLWS (Yagi et al., 2013). Furthermore, REMSAs confirmed that YLWS recognizes and binds to *ndhA* but not to *ndhB* and *rps14* transcripts (Figures S6B, S8).

Multiple organellar RNA editing factors (MORFs) are key components of editosomes, which edit plastid/mitochondrial RNAs in flowering plants (Takenaka et al., 2012). We tested if YLWS interacted with MORF proteins. Yeast-two-hybrid

assays showed that YLWS interacted with OsMORF8a (Os09g04670) and OsMORF8b (Os09g33480) in yeast, but not with OsMORF9 (Os08g04450), WSP1 (Os04g51280), or the negative control (Figure S6C). We examined the subcellular localization in rice protoplasts and found that OsMORF8a and OsMORF8b were partially located in chloroplasts (Figure S9). Further, bimolecular fluorescence complementation (BiFC) and luciferase complementation assays in *Nicotiana benthamiana* confirmed the interaction between YLWS and OsMORF8a (and OsMORF8b) *in vivo* (Figure S6D–F). These results suggested that YLWS could be involved in RNA editing via an editosome coupled with OsMORF8a/b.

DISCUSSION

YLWS is a P-type PPR protein that is essential for chloroplast development

We isolated and characterized a *ylws* mutant that showed a white-striped leaf phenotype during early seedling growth but later reverted to a normal green phenotype (Figure 1A–C). The *ylws* seedlings grown at 20°C were near-albino and the chlorophyll ultrastructure was seriously disrupted (Figures 1A, 2D–F). The *ylws* mutant displayed moderate white striping at 25°C and a pale-green phenotype at 30°C (Figure 1E). Correspondingly, the chlorophyll contents in *ylws* mutant seedlings relative to the WT were strongly reduced at 20°C but only slightly reduced at 30°C (Figure 1F–H). These results indicated that the *ylws* mutant phenotype was sensitive to low temperatures.

Chloroplast development requires coordinated expression of nuclear and plastid genes (Hedtko et al., 1997; Yu et al., 2014). Defects in PEP and NEP genes affect chloroplast development and reduce leaf pigmentation (Barkan and Small, 2014; Tang et al., 2017; Liu et al., 2018). The PEP complex consists of several nuclear-encoded proteins and four plastid-encoded core subunits (Steiner et al., 2011) and, to a certain extent, upregulation of NEP-associated genes is probably due to defects in the PEP complex in chloroplasts (Lv et al., 2017). PEP-dependent genes, such as *PsaA*, *PsaB*, and *RbcL*, in *ylws* mutant seedlings grown at 20°C, were downregulated, but NEP-dependent genes, such as *rpoA*, *rpoB*, *rpoC1*, and *rpoC2*, were upregulated (Figure 8A), implying that loss of function of YLWS impedes chloroplast PEP complex activity and that YLWS is required for the chloroplast PEP transcription machinery formation under low temperatures.

Impaired PEP activity and ribosome biosynthesis may cause the *ylws* phenotype

RNA splicing is the process of removing introns from pre-mRNAs and connecting exons to form a continuous mRNA molecule for translation. RNA-binding proteins play vital roles in splicing RNA introns in plant plastids (de Longevialle et al., 2010). PPRs function as RNA-binding proteins and are implicated in RNA processing, stabilization, cleavage, and

group II intron splicing (Barkan and Small, 2014). P-type PPR proteins are mainly responsible for intron splicing. In Arabidopsis, PBF2, EMB1270, and ECD2 belong to the P-subfamily. PBF2 is specifically required for *ycf3* intron 1 splicing (Wang et al., 2020), and EMB1270 interacts with CFM2 to splice specific group II introns in *clpP1.2*, *ycf3.1*, *ndhA*, and *ndhB* transcripts (Zhang et al., 2021). ECD2 also participates in the splicing of *ndhA*, *ycf3-int-1*, *rps12-int-2*, and *clpP-int-2* transcripts in cotyledon chloroplasts (Wang et al., 2021). In contrast with PPRs in Arabidopsis, few P-type PPRs have been cloned in rice, and the mechanisms of their post-transcriptional regulation of plastid genes remain unclear.

We identified a P-type PPR gene, YLWS, which has higher expression in leaves and its mutation caused white-striped leaves and abnormal chloroplast structure in seedlings (Figures 1–4). YLWS was localized in chloroplast nucleoids (Figure 4C, D), suggesting that YLWS was involved in post-transcriptional modification and translation. Further analyses demonstrated that YLWS participates in splicing *atpF*, *rpl2*, *ndhA*, and *rps12* transcripts during early seedling development (Figures 5, 6). Based on the reported method (Barkan et al., 2012; Yagi et al., 2013), we predicted the potential binding sites of YLWS (Figure S3). EMSA assays and RNA CoIP analysis in rice protoplast confirmed that YLWS targets specific sites in *ndhA*, *atpF*, and *rpl2* pre-mRNAs (Figures 7, S4). However, no specific predicted binding sequence was identified in the *rps12* intron. It is notable that we found multiple YLWS-binding sites in *ndhA* and *atpF* pre-mRNAs and, among these sites, the *ndhA*-3 and *atpF*-1 sites were located in the first exon of the respective pre-mRNAs (Figure 7A), suggesting that YLWS target sites are not confined to introns. Given that PPR proteins have stabilization, translation, splicing, and other unknown functions, YLWS may bind to exons of *ndhA* and *atpF* pre-mRNAs to perform other functions.

Among the abnormally spliced transcripts, *rps12* encodes the ribosomal protein S12, which is a component of the 30S ribosomal subunit, whereas *rpl2* encodes ribosomal protein subunit L2, which is involved in the peptidyl-transferase center. The absence of Rpl2 is a sensitive signal for a defective ribosomal function center (Nierhaus, 1982). Most studies on ribosome-deficient mutants have revealed that their proteins function in splicing by associating specifically with one or more group II introns. In Arabidopsis, EMB2654 is required for *trans*-splicing of *rps12* transcript, and its *emb2654* mutant lacked the Rps12 protein, thus failing to assemble the small subunit of the plastid ribosome (Aryamanesh et al., 2017). In maize, the *ppr4-1* mutant lacks chloroplast ribosomes because of the failure to splice the first intron of *rps12-intron 1* (Schmitz-Linneweber et al., 2006). Although *rps12* was spliced defectively in our study, no specific binding sequence was identified in the *rps12* intron; hence, the splicing defect of *rps12* was likely to be a secondary effect. WSL, WSL5, and CDE4 in rice are also involved in *rpl2* splicing, and all *wsl*, *wsl5*, and *cde4* mutants exhibit abnormal plastid transcriptional/translational machinery and defective chloroplast development (Tan et al., 2014; Liu et al., 2018; Liu et al., 2021). In addition, all

inefficient *rp12* splicing in barley, Arabidopsis, and rice results in ribosome-deficient plastids and albino phenotypes (Hess et al., 1994; Tan et al., 2014; Huang et al., 2018). Therefore, the low abundance of Rpl2 protein in the *ylws* mutant suggests that defective splicing of *rp12* probably caused ribosome-deficient plastids in the *ylws* mutant.

Although RNA pull-down analysis showed that YLWS binds to the 23S rRNA *in vitro*, REMSA analysis revealed that YLWS could not bind to predicted sites. 23S and 16S rRNA were significantly decreased in the *ylws* mutant at 20°C but not at 30°C (Figure S5). As the *ylws* mutant phenotype is temperature sensitive, we speculated that the deficiency of 23S and 16S rRNA was due to impaired ribosome biosynthesis caused by defective splicing of *rp12* transcript, but not the direct effect of the *ylws* mutation. In support, we found that when the editing site of *rps8* was impaired, the 23S and 16S rRNAs were also significantly decreased at 20°C but not at 30°C (Zhang et al., 2020). Many mutants that share similar characteristics of defective chloroplast ribosomes also have 23S and 16S rRNA deficiencies at low temperatures (20°C) (Wang et al., 2016; Zoschke et al., 2016; Liu et al., 2021).

In addition, *ndhA*, *ndhB*, and *rps14* transcripts were abnormally edited in the *ylws* mutant and we found that YLWS specifically recognized RNA sequences close to the editing sites of *ndhA* but not *rps14* and *ndhB* (Figure S6). Whereas YLWS might participate in the editing and splicing of *ndhA*, and given that knockout of the NDH complex in tobacco (*Nicotiana tabacum*) results in no phenotypic change under standard conditions, we speculated that *ndhA* and *ndhB* might not be responsible for the *ylws* mutant phenotype (Burrows et al., 1998). As no specific predicted binding sequence was identified in *ndhB* and *rps14* it is possible that the editing defect of *ndhB* and *rps14* is a secondary effect caused by the *ylws* mutation.

We further found that YLWS participates in both editing and splicing of *ndhA* and splicing of *rp12* by targeting specific recognition motifs (Figures 7, S6). Unlike the Arabidopsis PPR protein SOT1, which contains a crucial small SMR domain with endonuclease activity that can directly splice the rRNA (Zhou et al., 2017), YLWS does not have an SMR-like domain. In maize, PPR-E proteins function in RNA editing with the assistance of MORFs as key editing factors (Wang et al., 2023). YLWS also interacts with MORF proteins (Figure S6). Therefore, we speculated that YLWS mainly acts as a recognition protein to participate in splicing or editing RNAs complexed with other splicing or editing factors.

Our overall results support the view that splicing defects of *rp12* transcripts largely contributed to disrupting chloroplast protein translation by damaging the assembly of the plastid ribosome, leading to disrupted PEP activity, abnormal chloroplast development, and the albino phenotype of the *ylws* mutant.

CONCLUSIONS

Here, we report that YLWS, a P-type PPR protein, plays a vital role in chloroplast development. YLWS is involved in

chloroplast RNA splicing by targeting specific pre-mRNA sequences. YLWS influences plastid gene expression and plastid ribosome biogenesis. Identification of YLWS will help to elucidate the molecular mechanisms of plastid development and ribosome biogenesis and provides insight into the regulatory mechanism of chloroplast development in young seedlings.

MATERIALS AND METHODS

Plant materials and growth conditions

The *ylws* mutant was identified in an EMS-mutagenized population of *indica* rice cultivar Nanjing 11 (NJ11). Plants were grown in the field (natural long-day conditions) or growth chamber at 30, 25, and 20°C with a 16-h-light/8-h-darkness photoperiod. Third leaves of seedlings at ~15 d post planting were used for most analyses. Crosses were made between the *ylws* mutant and NJ11 for genetic analysis, and between the *ylws* mutant and line 02428 (*japonica*) for gene mapping.

Pigment contents and TEM

WT and *ylws* mutant seedlings were grown in growth chambers as described above. Fresh leaves were collected to determine the chlorophyll contents using a spectrophotometer as previously described (Arnon, 1949). Briefly, 0.2 g leaves were cut into pieces and soaked in 95% ethanol for 48 h in darkness with periodic gentle shaking. The supernatants were collected by centrifugation and analyzed using a spectrophotometer (Beckman Coulter, DU 800 UV/Vis, USA) at 665, 649, and 470 nm to determine Chl *a*, Chl *b*, and carotenoid contents, respectively.

TEM was performed as previously described (Wang et al., 2016). Briefly, leaves from the WT and green and white sectors of the *ylws* mutant were cut into 0.5-cm pieces and fixed in 2.5% glutaraldehyde in phosphate buffer (0.1 mol L⁻¹, pH 7.2) at 4°C for 4 h. Air bubbles on the surface of leaf blades were removed by a vacuum pump. The leaf blades were fixed in 1% OsO₄ at room temperature for 12 h and then incubated overnight at 4°C. The tissues were dehydrated in an ethanol series, infiltrated in a gradient series of epoxy resin, and finally embedded in Spurr's medium prior to ultrathin sectioning. Samples were stained again and then observed with a Hitachi H-7650 TEM.

Map-based cloning and plant transformation

Twenty F₂ plants with the recessive *ylws* phenotype from the cross between the *ylws* mutant and line 02428 (*japonica*) were used for preliminary mapping, and 983 F₂ plants with mutant phenotype were selected for fine mapping. InDel/new SSR markers were designed based on the 93-11 (*indica*) and Nipponbare (*japonica*) sequences posted at NCBI (<http://www.ncbi.nlm.nih.gov>). The YLWS locus was narrowed to a 148-kb genomic region flanked by markers L10 and L22 on the short arm of chromosome 3. Newly developed PCR-based molecular markers used for fine mapping are listed in Table S3.

For complementation tests of the *ylws* mutant, an ~4-kb WT genomic fragment containing the promoter, two exons, and one intron of *YLWS* was amplified and cloned into the pCubi-1390 binary vector. The pCubi-1390-*YLWS* plasmid was transformed into *ylws* mutant calli using *Agrobacterium tumefaciens* (strain EHA105).

To generate *YLWS* CRISPR/Cas9 lines, a 20-bp sgRNA targeting the first exon of *YLWS* was cloned into the CRISPR/Cas9 vector according to a previously described method (Miao et al., 2013). The plasmid was used to infect Kitaake calli using *A. tumefaciens*. Hygromycin-resistant calli were grown in a greenhouse to obtain transgenic plants. Positive transgenic plants were identified by PCR amplification and sequencing.

Subcellular localization of YLWS

The full-length *YLWS* coding sequence was amplified and cloned into the N terminus of the GFP tag of the PAN580-GFP vector driven by the CaMV35S promoter to generate the 35S::*YLWS*-GFP construct. The construct was transformed into rice protoplasts extracted from 9-d-old seedlings and incubated at 28°C for 16 h in darkness before the examination. GFP fluorescence was observed with a confocal laser scanning microscope (LSM 700; Zeiss).

RNA isolation, RT-PCR, and qRT-PCR analyses

Total RNA was extracted using a previously reported method (Lan et al., 2020) and reverse transcribed using PrimeScript II Reverse Transcriptase (TaKaRa) with an oligo(dT)18 primer for nuclear-encoded genes or random hexamer primers for plastid-encoded genes.

Real-time quantitative PCR was performed using a SYBR Premix Ex Taq Kit (TaKaRa) on an ABI Prism 7500 Real-Time PCR System. *UBQ5* (*LOC_Os03g13170*) was used as the reference gene. Specific primers for qRT-PCR are listed in Table S3. We performed three biological replicates for each experiment. Relative gene expression was analyzed using the $2^{-\Delta\Delta Ct}$ method (Livak and Schmittgen, 2001).

RNA CoIP

A 35S::*YLWS*-GFP construct was transformed into rice protoplasts extracted from 9-d-old NJ11 seedlings and incubated for 16 h in darkness at 28°C. RNA CoIP analysis was performed using an RNA Immunoprecipitation Kit (P0101, Gene Seed, Guangzhou) according to the instructions. Briefly, equal amounts of A + G protein beads were separately incubated with GFP antibody and IgG antibody in an incubation buffer and washed with a washing buffer. The protoplasts were lysed in lysis buffer supplemented with 1% RNase inhibitor and protease inhibitor for 10 min. After centrifuging at 4°C for 10 min the supernatant was divided into two parts and incubated with A + G protein beads, which bound the GFP and IgG antibodies in an incubation buffer. After incubation, the beads were washed three times with washing buffer. RNA that bound to the beads was extracted with reagents provided by the kit according to instructions provided with the kit. The RNA was reverse transcribed to cDNA for qPCR

analysis. The incubation buffer, lysis buffer, and washing buffer were provided by the kit. Normal anti-mouse IgG was used as a negative control. *rpl23*, *atpA*, and *ndhH* were used as *rpl2*-CK, *atpF*-CK, and *ndhA*-CK, respectively. To validate putative *YLWS*-binding targets, three biological replicates of immunoprecipitated RNA in chromatin immunoprecipitation (ChIP) were applied for each qPCR using the relevant primer pairs listed in Table S3. Relative enrichment was calculated using the $2^{-\Delta\Delta Ct}$ method (Livak and Schmittgen, 2001), and significant differences were evaluated by *t*-tests comparing IP samples and IgG controls.

RNA pull-down

The *YLWS* coding region was amplified and cloned into vector PGEX-4T-2. GST and *YLWS*-GST were expressed at 16°C with 0.5 mM IPTG for 16 h. The biotin-labeled 23S rRNA probe was *in vitro* transcribed and biotin labeled using T7 RNA polymerase (Gene Seed, catalog no. R0402). RNA pull-down assays were performed with a PureBinding™ RNA-Protein Pull-down Kit (Gene Seed, catalog no. P0201). The unlabeled and biotin-labeled 23S probes were incubated with Streptavidin Magnetic Beads for 30 min, followed by incubation with GST-*YLWS* protein for 1 h. The beads were washed six times with 1× phosphate-buffered saline buffer and boiled for 10 min, and the eluate was analyzed by western blot using an anti-GST antibody.

Protein extraction, SDS-PAGE, and immunodetection

Total protein was isolated from WT and *ylws* mutant leaves at the three-leaf stage using protein extraction buffer (50 mM Tris-HCl, pH 8.0, 1 mM MgCl₂, 10 mM EDTA, 0.5 M sucrose, 0.5 M DTT, and 1× protease inhibitor cocktail). The extracts were separated by sodium dodecyl sulfate-PAGE, transferred to nitrocellulose (NC) membranes, and immunoblotted with specific antibodies. Antibodies were obtained from BPI (<http://www.proteomics.org.cn>).

RNA analysis

Total RNA was extracted from leaves of 15-d-old WT and *ylws* plants grown at 20°C or 30°C using an RNAprep Pure Plant Mini Kit (TIANGEN, Beijing). RNA samples were diluted to 200 ng/μL. RNA analysis was performed following the Agilent RNA 6000 Nano Kit instructions.

RNA editing sites and RNA splicing analyses

Specific cDNA fragments for RNA editing were amplified with primers following previously published protocols (Takenaka and Brennicke, 2007) and compared to identify the C-to-T RNA editing efficiency. The primers used for RNA editing analysis were obtained from a previous study (Tan et al., 2014).

For RNA splicing analysis, we designed primers flanking the introns to amplify plastid genes with at least one intron (Table S3). PCR cycles were adjusted to between 25 and 35 according to the corresponding gene expression.

Northern blotting

Total RNA from WT and *ylws* mutant plants was isolated from leaves of three-leaf-stage seedlings using *TransZol* Up

YLWS regulates rice chloroplast development

(TransGen); ~2 mg RNA was fractionated in a 1.5% (w/v) denaturing formaldehyde agarose gel and transferred onto Hybond NC nylon membranes (GE Healthcare Biosciences). Probes for northern blotting were labeled using the DIG Northern Starter Kit (Roche) according to the instruction manual. Primers are listed in Table S3.

Prehybridization and hybridization were conducted at 68°C in PerfectHyb Plus Hybridization Buffer (Sigma) for 1 and 10 h, respectively. RNA was detected using the DIG Wash and Block Buffer Set (Roche) and finally imaged on an imaging system (Tanon 5200, LI-COR, Beijing).

EMSA

The 5'-biotin-labeled probes were synthesized by GenScript (Nanjing) (primer pairs listed in Table S3). The YLWS coding region was amplified and cloned into vector PGEX-4T-2. YLWS-GST was expressed at 16°C with 0.5 mM IPTG for 16 h. RNA-EMSA was performed using a Light Shift EMSA Kit following the manufacturer's recommendations. The 20 µL DNA binding reaction comprised 2 µL probe, 2 µL binding buffer, 1 µg purified GST or YLWS-GST protein, labeled probes or competitive probes, and RNase-free water. The samples were incubated at room temperature for 30 min, separated on native polyacrylamide gels containing 6.5% acrylamide, transferred onto a nylon membrane (Millipore, Billerica, USA), and crosslinked at 120 mJ/cm² using UV light. The membrane was incubated in 20 mL blocking buffer for 15 min and conjugate/blocking buffer solution for 15 min. Substrate equilibration buffer was applied to the membrane for 5 min after washing. Finally, the substrate working solution was added to detect the signal.

Bimolecular fluorescence complementation assay

YLWS-cYFP, MORF8a-nYFP, MORF8b-nYFP, and corresponding empty vectors were transformed into *A. tumefaciens* strain EHA105. For transient expression, *A. tumefaciens* carrying the different combinations was co-infiltrated into *Nicotiana benthamiana* leaves. After 48 h, the fluorescence was observed with an LSM700 confocal laser scanning microscope (Zeiss).

Firefly luciferase complementation assay

The YLWS coding sequence was fused to the pCAMBIA1300split_cLUC vector. The MORF8a and MORF8b coding sequences were fused to the pCAMBIA1300split_nLUC vector. Primers for these constructs are listed in Table S3. MORF8a-nLUC, MORF8b-nLUC, YLWS-cLUC, and corresponding empty vectors were transformed into *A. tumefaciens* strain EHA105. Different combinations of *A. tumefaciens* containing the above plasmids were co-transformed into *N. benthamiana* leaves. After 48 h, luciferase intensity was measured using a Night SHADE LB 985 imaging apparatus.

Accession numbers

Sequence data from this article can be found in the GenBank database under the following accession numbers: *FLO10*,

LOC_Os03g07220; *FLO18*, LOC_Os07g48850; *OGR1*, LOC_Os12g17080; *MPP25*, LOC_Os04g51350; *OsV4*, LOC_Os04g39970; *WSL*, LOC_Os01g37870; *ALS3*, LOC_Os01g48380; *OspTAC2*, LOC_Os03g60910; *OsPPR6*, LOC_Os05g49920; *WSL4*, LOC_Os02g35750; *WSL5*, LOC_Os04g58780; *UBQ5*, LOC_Os03g13170; *EMB1270*, AT3G18110; *PBF2*, AT3G42630; *ECD2*, AT5G50280; *WSP1*, LOC_Os04g51280; *OsMORF8a*, LOC_Os09g04670; *OsMORF8b*, LOC_Os09g33480; *OsMORF9*, LOC_Os08g04450; and *YSS1*, LOC_Os04g59570.

ACKNOWLEDGEMENTS

This work was supported by the Key Laboratory of Biology, Genetics, and Breeding of Japonica Rice in the Mid-lower Yangtze River, Ministry of Agriculture, China; Jiangsu Plant Gene Engineering Research Center; and Jiangsu Collaborative Innovation Center for Modern Crop Production. This research was also supported by grants from the National Natural Science Foundation (92035301), Jiangsu Science and Technology Development Program (BE2021360), Jiangsu Agricultural Science and Technology Innovation Fund Project (SCX (19)1079), and the Fundamental Research Funds for the Central Universities (JCQY201902).

CONFLICTS OF INTEREST

The authors have no conflicts of interest to declare.

AUTHOR CONTRIBUTIONS

J.M.W., Q.B.L., and C.L.Z. designed the experiments; J.L. and C.L.Z. performed the experiments; J.L. and Q.B.L. wrote the manuscript. Other authors assisted in experiments and discussed the results. All authors read and approved this manuscript.

Edited by: Congming Lu, Shandong Agricultural University, China

Received Dec. 10, 2022; **Accepted** Mar. 7, 2023; **Published** Mar. 10, 2023

REFERENCES

- Arnon, D.I.** (1949). Copper enzymes in isolated chloroplasts. Polyphenoloxidase in *Beta Vulgaris*. *Plant Physiol.* **24**: 1–15.
- Aryamanesh, N., Ruwe, H., Sanglard, L.V.P., Eshraghi, L., Bussell, J.D., Howell, K.A., Small, I., and des Francs-Small, C.C.** (2017). The pentatricopeptide repeat protein EMB2654 is essential for trans-splicing of a chloroplast small ribosomal subunit transcript. *Plant Physiol.* **173**: 1164–1176.
- Barkan, A., Rojas, M., Fujii, S., Yap, A., Chong, Y.S., Bond, C.S., and Small, I.** (2012). A combinatorial amino acid code for RNA recognition by pentatricopeptide repeat proteins. *PLoS Genet.* **8**: e1002910.

- Barkan, A., and Small, I.** (2014). Pentatricopeptide repeat proteins in plants. *Annu. Rev. Plant Biol.* **65**: 415–442.
- Burrows, P.A., Sazanov, L.A., Svab, Z., Maliga, P., and Nixon, P.J.** (1998). Identification of a functional respiratory complex in chloroplasts through analysis of tobacco mutants containing disrupted plastid *ndh* genes. *EMBO J.* **17**: 868–876.
- Cai, M.J., Li, S.Z., Sun, F., Sun, Q., Zhao, H.L., Ren, X.M., Zhao, Y.X., Tan, B.C., Zhang, Z.X., and Qiu, F.Z.** (2017). *Emp10* encodes a mitochondrial PPR protein that affects the cis-splicing of *nad2* intron 1 and seed development in maize. *Plant J.* **91**: 132–144.
- Chateigner-Boutin, A.L., des Francs-Small, C.C., Delannoy, E., Kahlau, S., Tanz, S.K., de Longevialle, A.F., Fujii, S., and Small, I.** (2011). OTP70 is a pentatricopeptide repeat protein of the E subgroup involved in splicing of the plastid transcript *rpoC1*. *Plant J.* **65**: 532–542.
- Corneille, S., Lutz, K., and Maliga, P.** (2000). Conservation of RNA editing between rice and maize plastids: Are most editing events dispensable? *Mol. Gen. Genet.* **264**: 419–424.
- Cui, X.A., Wang, Y.W., Wu, J.X., Han, X., Gu, X.F., Lu, T.G., and Zhang, Z.G.** (2019). The RNA editing factor DUA1 is crucial to chloroplast development at low temperature in rice. *New Phytol.* **221**: 834–849.
- de Longevialle, A.F., Small, I.D., and Lurin, C.** (2010). Nuclearily encoded splicing factors implicated in RNA splicing in higher plant organelles. *Mol. Plant* **3**: 691–705.
- de Souza, A., Wang, J.Z., and Dehesh, K.** (2017). Retrograde signals: Integrators of interorganellar communication and orchestrators of plant development. *Annu. Rev. Plant Biol.* **68**: 85–108.
- Gong, X.D., Su, Q.Q., Lin, D.Z., Jiang, Q., Xu, J.L., Zhang, J.H., Teng, S., and Dong, Y.J.** (2014). The rice *OsV4* encoding a novel pentatricopeptide repeat protein is required for chloroplast development during the early leaf stage under cold stress. *J. Integr. Plant Biol.* **56**: 400–410.
- Hammani, K., Okuda, K., Tanz, S.K., Chateigner-Boutin, A.L., Shikanai, T., and Small, I.** (2009). A study of new Arabidopsis chloroplast RNA editing mutants reveals general features of editing factors and their target sites. *Plant Cell* **21**: 3686–3699.
- Hammani, K., Takenaka, M., Miranda, R., and Barkan, A.** (2016). A PPR protein in the PLS subfamily stabilizes the 5'-end of processed *rpl16* mRNAs in maize chloroplasts. *Nucleic Acids Res.* **44**: 4278–4288.
- Hedtke, B., Borner, T., and Weihe, A.** (1997). Mitochondrial and chloroplast phage-type RNA polymerases in Arabidopsis. *Science* **277**: 809–811.
- Hess, W.R., Hoch, B., Zeltz, P., Hubschmann, T., Kossel, H., and Borner, T.** (1994). Inefficient *rpl2* splicing in barley mutants with ribosome-deficient plastids. *Plant Cell* **6**: 1455–1465.
- Hiratsuka, J., Shimada, H., Whittier, R., Ishibashi, T., Sakamoto, M., Mori, M., Kondo, C., Honji, Y., Sun, C.R., Meng, B.Y. et al.** (1989). The complete sequence of the rice (*Oryza sativa*) chloroplast genome: Intermolecular recombination between distinct tRNA genes accounts for a major plastid DNA inversion during the evolution of the cereals. *Mol. Gen. Genet.* **217**: 185–194.
- Huang, W.H., Zhu, Y.J., Wu, W.J., Li, X., Zhang, D.L., Yin, P., and Huang, J.R.** (2018). The pentatricopeptide repeat protein SOT5/EMB2279 is required for plastid *rpl2* and *trnK* intron splicing. *Plant Physiol.* **177**: 684–697.
- Kim, S.R., Yang, J.I., Moon, S., Ryu, C.H., An, K., Kim, K.M., Yim, J., and An, G.** (2009). Rice *OGR1* encodes a pentatricopeptide repeat-DYW protein and is essential for RNA editing in mitochondria. *Plant J.* **59**: 738–749.
- Lan, J., Lin, Q., Zhou, C., Ren, Y., Liu, X., Miao, R., Jing, R., Mou, C., Nguyen, T., Zhu, X. et al.** (2020). Small grain and semi-dwarf 3, a WRKY transcription factor, negatively regulates plant height and grain size by stabilizing SLR1 expression in rice. *Plant Mol. Biol.* **104**: 429–450.
- Liu, X., Lan, J., Huang, Y., Cao, P., Zhou, C., Ren, Y., He, N., Liu, S., Tian, Y., Nguyen, T. et al.** (2018). WSL5, a pentatricopeptide repeat protein, is essential for chloroplast biogenesis in rice under cold stress. *J. Exp. Bot.* **69**: 3949–3961.
- Liu, X., Zhang, X., Cao, R., Jiao, G., Hu, S., Shao, G., Sheng, Z., Xie, L., Tang, S., Wei, X. et al.** (2021). *CDE4* encodes a pentatricopeptide repeat protein involved in chloroplast RNA splicing and affects chloroplast development under low-temperature conditions in rice. *J. Integr. Plant Biol.* **63**: 1724–1739.
- Livak, K.J., and Schmittgen, T.D.** (2001). Analysis of relative gene expression data using real-time quantitative PCR and the $2^{-\Delta\Delta CT}$ method. *Methods* **25**: 402–408.
- Lu, Y., Li, C., Wang, H., Chen, H., Berg, H., and Xia, Y.** (2011). AtPPR2, an Arabidopsis pentatricopeptide repeat protein, binds to plastid 23S rRNA and plays an important role in the first mitotic division during gametogenesis and in cell proliferation during embryogenesis. *Plant J.* **67**: 13–25.
- Lurin, C., Andres, C., Aubourg, S., Bellaoui, M., Bitton, F., Bruyere, C., Caboche, M., Debast, C., Gualberto, J., Hoffmann, B. et al.** (2004). Genome-wide analysis of Arabidopsis pentatricopeptide repeat proteins reveals their essential role in organelle biogenesis. *Plant Cell* **16**: 2089–2103.
- Lv, Y., Shao, G., Qiu, J., Jiao, G., Sheng, Z., Xie, L., Wu, Y., Tang, S., Wei, X., and Hu, P.** (2017). *White Leaf and Panicle 2*, encoding a PEP-associated protein, is required for chloroplast biogenesis under heat stress in rice. *J. Exp. Bot.* **68**: 5147–5160.
- Miao, J., Guo, D.S., Zhang, J.Z., Huang, Q.P., Qin, G.J., Zhang, X., Wan, J.M., Gu, H.Y., and Qu, L.J.** (2013). Targeted mutagenesis in rice using CRISPR-Cas system. *Cell Res.* **23**: 1233–1236.
- Moreira, D., Le Guyader, H., and Philippe, H.** (2000). The origin of red algae and the evolution of chloroplasts. *Nature* **405**: 69–72.
- Nierhaus, K.H.** (1982). Structure, assembly, and function of ribosomes. *Curr. Top. Microbiol. Immunol.* **97**: 81–155.
- O'Toole, N., Hattori, M., Andres, C., Iida, K., Lurin, C., Schmitz-Linneweber, C., Sugita, M., and Small, I.** (2008). On the expansion of the pentatricopeptide repeat gene family in plants. *Mol. Biol. Evol.* **25**: 1120–1128.
- Pfalz, J., Liere, K., Kandlbinder, A., Dietz, K.J., and Oelmüller, R.** (2006). PTAC2, -6, and -12 are components of the transcriptionally active plastid chromosome that are required for plastid gene expression. *Plant Cell* **18**: 176–197.
- Schmitz-Linneweber, C., Williams-Carrier, R.E., Williams-Voelker, P. M., Kroeger, T.S., Vichas, A., and Barkan, A.** (2006). A pentatricopeptide repeat protein facilitates the trans-splicing of the maize chloroplast *rps12* pre-mRNA. *Plant Cell* **18**: 2650–2663.
- Shikanai, T., and Fujii, S.** (2013). Function of PPR proteins in plastid gene expression. *RNA Biol.* **10**: 1446–1456.
- Steiner, S., Schroter, Y., Pfalz, J., and Pfanschmidt, T.** (2011). Identification of essential subunits in the plastid-encoded RNA polymerase complex reveals building blocks for proper plastid development. *Plant Physiol.* **157**: 1043–1055.
- Su, N., Hu, M.L., Wu, D.X., Wu, F.Q., Fei, G.L., Lan, Y., Chen, X.L., Shu, X.L., Zhang, X., Guo, X.P. et al.** (2012). Disruption of a rice pentatricopeptide repeat protein causes a seedling-specific albino phenotype and its utilization to enhance seed purity in hybrid rice production. *Plant Physiol.* **159**: 227–238.
- Sugimoto, H., Kusumi, K., Tozawa, Y., Yazaki, J., Kishimoto, N., Kikuchi, S., and Iba, K.** (2004). The virescent-2 mutation inhibits translation of plastid transcripts for the plastid genetic system at an early stage of chloroplast differentiation. *Plant Cell Physiol.* **45**: 985–996.
- Takenaka, M., and Brennicke, A.** (2007). RNA editing in plant mitochondria: Assays and biochemical approaches. *Methods Enzymol.* **424**: 439–458.
- Takenaka, M., Zehrmann, A., Verbitskiy, D., Hartel, B., and Brennicke, A.** (2013). RNA editing in plants and its evolution. *Annu. Rev. Genet.* **47**: 335–352.
- Takenaka, M., Zehrmann, A., Verbitskiy, D., Kugelman, M., Hartel, B., and Brennicke, A.** (2012). Multiple organellar RNA editing factor

- (MORF) family proteins are required for RNA editing in mitochondria and plastids of plants. *Proc. Nat. Acad. Sci. U.S.A.* **109**: 5104–5109.
- Tan, J., Tan, Z., Wu, F., Sheng, P., Heng, Y., Wang, X., Ren, Y., Wang, J., Guo, X., Zhang, X. et al.** (2014). A novel chloroplast-localized pentatricopeptide repeat protein involved in splicing affects chloroplast development and abiotic stress response in rice. *Mol. Plant* **7**: 1329–1349.
- Tang, J., Zhang, W., Wen, K., Chen, G., Sun, J., Tian, Y., Tang, W., Yu, J., An, H., Wu, T. et al.** (2017). OsPPR6, a pentatricopeptide repeat protein involved in editing and splicing chloroplast RNA, is required for chloroplast biogenesis in rice. *Plant Mol. Biol.* **95**: 345–357.
- Toda, T., Fujii, S., Noguchi, K., Kazama, T., and Toriyama, K.** (2012). Rice *MPPR25* encodes a pentatricopeptide repeat protein and is essential for RNA editing of *nad5* transcripts in mitochondria. *Plant J.* **72**: 450–460.
- Wang, D.K., Liu, H.Q., Zhai, G.W., Wang, L.S., Shao, J.F., and Tao, Y.Z.** (2016). *OspTAC2* encodes a pentatricopeptide repeat protein and regulates rice chloroplast development. *J. Genet. Genomics* **43**: 601–608.
- Wang, X.M., Yang, Z.P., Zhang, Y., Zhou, W., Zhang, A.H., and Lu, C.M.** (2020). Pentatricopeptide repeat protein PHOTOSYSTEM I BIOGENESIS FACTOR2 is required for splicing of *ycf3*. *J. Integr. Plant Biol.* **62**: 1741–1761.
- Wang, X.W., An, Y.Q., Qi, Z., and Xiao, J.W.** (2021). PPR protein early chloroplast development 2 is essential for chloroplast development at the early stage of Arabidopsis development. *Plant Sci.* **308**: 110908.
- Wang, Y., Li, H., Huang, Z.Q., Ma, B., Yang, Y.Z., Xiu, Z.H., Wang, L., and Tan, B.C.** (2023). Maize PPR-E proteins mediate RNA C-to-U editing in mitochondria by recruiting the trans deaminase PCW1. *Plant Cell* **35**: 529–551.
- Wang, Y., Wang, C., Zheng, M., Lyu, J., Xu, Y., Li, X., Niu, M., Long, W., Wang, D., Wang, H. et al.** (2016). WHITE PANICLE1, a val-tRNA synthetase regulating chloroplast ribosome biogenesis in rice, is essential for early chloroplast development. *Plant Physiol.* **170**: 2110–2123.
- Williams, P.M., and Barkan, A.** (2003). A chloroplast-localized PPR protein required for plastid ribosome accumulation. *Plant J.* **36**: 675–686.
- Wu, M.M., Ren, Y.L., Cai, M.H., Wang, Y.L., Zhu, S.S., Zhu, J.P., Hao, Y. Y., Teng, X., Zhu, X.P., Jing, R.N. et al.** (2019). Rice *FLOURY ENDOSPERM10* encodes a pentatricopeptide repeat protein that is essential for the trans-splicing of mitochondrial *nad1* intron 1 and endosperm development. *New Phytol.* **223**: 736–750.
- Yagi, Y., Hayashi, S., Kobayashi, K., Hirayama, T., and Nakamura, T.** (2013). Elucidation of the RNA recognition code for pentatricopeptide repeat proteins involved in organelle RNA editing in plants. *PLoS ONE* **8**: e57286.
- Yu, M.Z., Wu, M.M., Ren, Y.L., Wang, Y.H., Li, J.F., Lei, C.L., Sun, Y.L., Bao, X.H., Wu, H.M., Yang, H. et al.** (2021). Rice *FLOURY ENDOSPERM 18* encodes a pentatricopeptide repeat protein required for 5' processing of mitochondrial *nad5* messenger RNA and endosperm development. *J. Integr. Plant Biol.* **63**: 834–847.
- Yu, Q.B., Huang, C., and Yang, Z.N.** (2014). Nuclear-encoded factors associated with the chloroplast transcription machinery of higher plants. *Front. Plant Sci.* **5**: 316.
- Zhang, J., Guo, Y., Fang, Q., Zhu, Y., Zhang, Y., Liu, X., Lin, Y., Barkan, A., and Zhou, F.** (2020). The PPR-SMR protein ATP4 is required for editing the chloroplast *rps8* mRNA in rice and maize. *Plant Physiol.* **184**: 2011–2021.
- Zhang, J., Xiao, J.W., Li, Y.Q., Su, B.D., Xu, H.M., Shan, X.Y., Song, C.W., Xie, J.B., and Li, R.L.** (2017). PDM3, a pentatricopeptide repeat-containing protein, affects chloroplast development. *J. Exp. Bot.* **68**: 5615–5627.
- Zhang, L., Chen, J., Zhang, L., Wei, Y., Li, Y., Xu, X., Wu, H., Yang, Z.N., Huang, J., Hu, F. et al.** (2021). The pentatricopeptide repeat protein EMB1270 interacts with CFM2 to splice specific group II introns in Arabidopsis chloroplasts. *J. Integr. Plant Biol.* **63**: 1952–1966.
- Zhou, K., Ren, Y., Zhou, F., Wang, Y., Zhang, L., Lyu, J., Wang, Y., Zhao, S., Ma, W., Zhang, H. et al.** (2017). *Young Seedling Stripe1* encodes a chloroplast nucleoid-associated protein required for chloroplast development in rice seedlings. *Planta* **245**: 45–60.
- Zoschke, R., Watkins, K.P., Miranda, R.G., and Barkan, A.** (2016). The PPR-SMR protein PPR53 enhances the stability and translation of specific chloroplast RNAs in maize. *Plant J.* **85**: 594–606.

SUPPORTING INFORMATION

Additional Supporting Information may be found online in the supporting information tab for this article: <http://onlinelibrary.wiley.com/doi/10.1111/jipb.13477/supinfo>

Figure S1. Multiple sequence alignments of YLWS protein and putative homologs

Figure S2. Expression level of YLWS during the panicle development stage

Figure S3. Prediction of potential YLWS-binding sites

Figure S4. EMSA analysis of YLWS protein

Figure S5. Analysis of 23S rRNA

Figure S6. YLWS affects RNA editing by forming an editosome with MORFs

Figure S7. Analysis of other 18 RNA editing sites in WT and *ylws* mutant (white-striped sectors)

Figure S8. REMSA analysis of YLWS protein

Figure S9. Subcellular localization of OsMORF8a and OsMORF8b

Table S1. Phenotypic segregation in reciprocal crosses between WT and the *ylws* mutant

Table S2. Editing efficiencies of 21 identified RNA editing sites in rice chloroplast RNA

Table S3. Primers used in this study



Scan using WeChat with your smartphone to view JIPB online



Scan with iPhone or iPad to view JIPB online